Analytical Methods

Accepted Manuscript

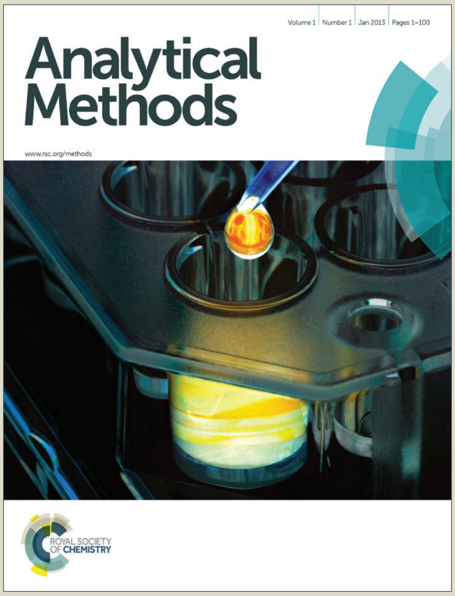
Volume 1 | Number 1 | Jan 2013 | Pages 1–100

Analytical Methods

www.rsc.org/methods

ROYAL SOCIETY OF CHEMISTRY

www.rsc.org/methods

High sensitive simultaneous electrochemical determination of hydroquinone, catechol and resorcinol based on carbon dots/reduced graphene oxide composite modified electrode

Wuxiang Zhang[a], Jianzhong Zheng[a], Zhongqiu Lin[a], Ling Zhong[a], Jiangu Shi[a],
Chan Wei[a], Hanqiang Zhang[a], Aiyou Hao[b], Shirong Hu[a, b*]

[a] College of Chemistry and Environment, Minnan Normal University,
Zhangzhou 363000, P.R. China.

[b] School of Chemistry and Chemical Engineering, Shandong University,
Jinan 250100, P.R. China.

---

* Corresponding author: Tel.: +86 596 2528075. Fax: +86 596 2528075

E-mail address: Hushirong6666@163.com (prof. S. Hu).

Abstract In this work, a simple and highly sensitive electrochemical method was developed for the simultaneous detection of hydroquinone (HQ), catechol (CC) and resorcinol (RC) based on carbon dots/reduced graphene oxide composite on the glassy carbon electrode (GCE). The electron communication between reduced graphene oxide (r-GO) and CDs can be further strengthened *via* hydrogen bonding and π-π stacking force. The electrochemical behavior of CDs/r-GO/GCE sensor toward HQ, CC and RC as probed by cyclic voltammetry (CV) and Differential pulse voltammetry (DPV). Results showed that the calibration curves were in the range of 0.5 to 1000 μM, 1.0 to 950 μM and 5.0 to 600 μM, respectively. With the detection limits for HQ, CC and RC were 0.17 μM, 0.28 μM and 1.0 μM (S/N=3), respectively. Moreover, the sensor has successfully applied in detecting tap water, river water and industrial sewage.

Keywords Carbon dots; Reduced graphene oxide; Simultaneous detection; Dihydroxybenzene isomers

1. Introduction

As the dihydroxybenzene isomers, hydroquinone (HQ), catechol (CC) and resorcinol (RC) are derived from a wealth of sources, including agriculture, factory discharges, wastewater treatment plants and other related industries.[1-3] Owing to their low degradation in environment and high toxicity to environment and human, the US Environment Protection Agency (EPA) and the European Union have placed dihydroxybenzene isomers as environment pollutants.[4] Therefore simultaneous determination of dihydroxybenzene isomers has become a hot topic for scientists.[5] By now, chromatography,[6-7] spectrophotometry[8] and electrochemical methods have been designed for the simultaneous detection of dihydroxybenzene isomers. Among these methods, electrochemical detection is the most promising technology because of many intrinsic advantages such as rapid response, high sensitivity and low cost.[9-10] However, the key problem for simultaneously detecting HQ, CC and RC here is the interference with each other and their peak currents are overlapped at conventional electrodes.[11] In this context, it is particularly urgent to explore a novel electrode material to modify glassy carbon electrode (GCE) for simultaneous determination of dihydroxybenzene isomers.

Graphene, which is a single atomic sheet of the conjugated sp^2 carbon atoms, has been extensively studied due to its excellent characteristics with large surface structure, good mechanical strength, high electronic conductivity and chemical stability.[12-15] Moreover, many potential applications and unique properties of graphene can be realized by integrating them into more complex assemblies. The synergetic effect not only exhibits their excellent charge transport rate, but also reduces graphene-supported hybrids material interfacial defect.[16-19] Notably, many graphene-based composite chemicals have developed to detection of dihydroxybenzene isomers, including cadmium sulphide/reduced graphene oxide nanocomposite,[20] gold-graphene nanocomposite,[21] reduced graphene oxide-multiwall carbon nanotubes,[22] tungsten sulfide-graphene nanocomposite.[23] All these studies indicated that graphene with composite nanomaterials could efficiently improve the performance of sensor. In order to enrich the potential applications, the doping of other materials into graphene is the efficient way to enhance the electrochemical effects. Carbon dots (CDs), as a new class of “zero-dimensional” carbon material, has recently attracted much attention for a variety of purposes and applications, especially for their potential applications in fluorescence, biosensors and imaging.[24-27] Compared with conventional semiconductor quantum dots, CDs has the advantage in terms of biocompatibility, cytotoxicity and conductivity.[28-29] The existence of sp^2 (graphitic) π bonds gives it better charge-charge transport and oxidation-reduction performance.[30-31] Thus, to develop a novel CDs based materials is a strong challenging goal to determination of dihydroxybenzene isomers in these years. So we synthesized CDs with the method of reflux and applied carbon dots/reduced graphene oxide composites in electrochemical techniques for determination of dihydroxybenzene isomers.

In this work, a novel sensor of carbon dots/reduced graphene oxide (CDs/r-GO) was constructed to detect HQ, CC and RC for the first time. The peak oxidation potentials of the dihydroxybenzene isomers are separated by differential pulse voltammetry (DPV). The calibration curves for HQ, CC and RC were obtained in the range of 0.5 to 1000 μM, 1.0 to 950 μM and 5.0 to 600 μM, respectively. With the low limits of detection for HQ, CC and RC were 0.17 μM, 0.28 μM and 1.0 μM (S/N = 3). Furthermore, the CDs/r-GO modified electrode has been applied for the simultaneous determination of HQ, CC and RC in practical water samples.

2. Experimental

2.1. Reagents and apparatus

Citric acid, sodium hydroxide, sodium borohydride and phosphate buffer solution were purchased from Sinopharm Chemical Reagent Co., Ltd. Hydroquinone, catechol and resorcinol were obtained from Xilong Chemical Co., Ltd. All reagents were analytical grade reagents. All chemicals and solvents were used as received. All aqueous solutions were prepared using ultrapure water (18 MΩ·cm) from a Milli-Q system (Millipore). Scanning electron microscopy (SEM) was conducted on JEM-6010La (JEOL Japan) operating at 20 kV. Transmission electron microscopy (TEM) was performed on a FEI Tecnai G20 electron microscope operating at 300 kV (FEI Company, USA). The surface topography was observed with Atomic Force Microscopy (CSPM5500, China). UV-vis spectroscopy was registered by UV-1800PC spectrophotometer (Shanghai Mapada Instruments Co., Ltd, China). Fourier transform infrared (FT-IR) spectroscopy was obtained on Thermo NICOLET iS 10 (Thermo Fisher Scientific, America), operating spectrophotometer between 500 cm^{-1} and 4000 cm^{-1}. Fluorescence was obtained by a Varian Cary Eclipse fluorescence spectrophotometer (Agilent Technologies, America). Electrochemical measurements were performed on a CHI660E electrochemical workstation. The glassy carbon electrode was used as working electrode (CHI104). The Ag/AgCl electrode and platinum wire were used as reference and auxiliary electrodes, respectively.

2.2. Synthesis of carbon dots/reduced graphene oxide materials

Carbon dots (CDs) was synthesized by 2.0 g citric acid and 10 mL distilled water in a 50 mL round-bottom flask reflux heating at 200 ± 5 °C under magnetic stirring until producing the CDs with yellow-black. Lastly, the CDs was dialyzed for 24 h with the dialysis membranes of 1000 cutoffs and diluted to 50.00 mL volumetric flask with water, then stored at 4 °C ready for using. Graphene oxide (GO) was synthesized by oxidation of graphite using Hummers' method.[32] The CDs/r-GO was fabricated as follows: First, 4.0 mg of the obtained dry GO was ultrasonically redispersed into 20.00 mL deionized water, then 2.00 mL of the as-obtained CDs was dissolved in the obtained dispersion for 20 min by sonication in a water bath (KQ2200DE, 40 kHz). The suspension was moved in a 50 mL round-bottom flask under mechanically stirred. After that, 2.0 mg sodium borohydride was added into the suspension when the suspension was heated up to 80 °C and kept this temperature for 2 hours. The CDs/r-GO was obtained.

2.3. Modification of electrodes

Alumina powders with different sizes (1.0, 0.3 and 0.05 μm) were used to polish GCE before using. As-synthesed material (1.0 mg) was dispersed in 1mL of chitosan solution (0.5 wt.%) by ultra sonication to enhance the tackiness and selectivity of electrode.[33] Then, 8.0 μL of the suspension was dropped on the surface of GCE and dried in an oven at 60 °C for 20 min.

3. Results and discussion

3.1. Characterization of GO, CDs and CDs/r-GO composite

The surface morphologies of GO and CDs/r-GO were investigated by scanning electron microscope (SEM). As shown in **Fig. 1A**, the morphology of the GO layer resemble a thin wrinkled paper.[34] Transmission electron microscopy (TEM) image of the obtained CDs in **Fig. 1B**, these small CDs were well dispersed with a diameter of about 2.32 ± 0.8 nm, which was consistent with previous reports.[35] The inset in **Fig. 1B** shows the particle size distribution. Then **Fig. 1C** observed the crumpled graphene sheets were randomly aggregated and overlapped with each other, forming the characteristic of CDs/r-GO.

Fig. 1

Atomic force microscope (AFM) is a suitable instrument to evaluate topography of material. The GO/GCE (**Fig. 2A**), CDs/GCE (**Fig. 2B**) and CDs/r-GO/GCE (**Fig. 2C**) were used to explain the structures of the modified electrodes. It is observed that the surface of GO/GCE was hillock-like surface morphology and relatively smooth with an average roughness of 0.85 nm. The regular tapered convex surface of CDs/GCE and average roughness of was 2.34 nm. The irregular spinous islands and adjacent peaks on the CDs/r-GO/GCE and the average roughness was 14.30 nm, which indicated the surface morphology changed the roughness of each surface, and the GO, CDs and CDs/r-GO had been successfully modified on the electrodes. The change mechanism of topographies may be as follows: In reduction process of graphene oxide, the covalent bond and layered structure were destroyed, r-GO in different sections of materials, mutually stacked and the heaped. In addition, CDs attached between the r-GO layers could also increase the roughness of the composite.

Fig. 2

The optical properties of CDs are shown in **Fig. 3A**. The obvious absorption feature of UV-vis absorption spectrum were at approximately 226 nm and 275 nm, which were ascribed to the π–π^* transition of C=C in amorphous carbon systems.[36] The typical characteristics of GO peak are at 230 nm and 300 nm, consistent with previous report.[37] In contrast, there is a weak absorption peak of the CDs/r-GO at 260 nm ascribable to the CDs reacted with GO to obtain CDs/r-GO. The photoluminescence spectra in **Fig. 3A** suggest that the excitation wavelength of the emission spectrum was 446 nm and the emission wavelength of the excitation spectrum was 530 nm. The photoluminescence properties of CDs mainly attributed to size differences.[38] The functional groups were further characterized by FT-IR spectroscopy. As seen from the comparison between **Fig. 3B**, due to the existence of negative charge carboxyl and hydroxyl groups on the surface of CDs, the peak at 1713 cm^{-1}, 1403 cm^{-1} and 1202 cm^{-1} were assigned to the carbonyl/benzodiazepines characteristic vibrations of C=O, C=C and C-OH (phenolic) stretching bonds, respectively. The FT-IR peaks at 3400 and 3500 cm^{-1} are attributed to the stretching vibrations of O-H. The GO peak was at 2900 cm^{-1}, which is assigned to C-H bonds of sp^3 hybrid carbon, while the peak at 1050~1465 cm^{-1} indicates the existence of epoxy, C-O and C=C bonds.[39]

It was obviously seen that the peak intensity of C-O, C=C and C=O were much weaker in CDs/r-GO materials, which indicates that most of the oxygen-containing groups were removed after the reaction and the composite CDs/r-GO was achieved.

Fig. 3

3.2. Electrochemical behavior of dihydroxybenzene isomers

Cyclic voltammetry (CV) and electrochemical impedance spectroscopy (EIS) were exploited signal amplification capability of the different electrodes in a 1.0 mM $[Fe(CN)_6]^{3-/4-}$and 0.1 M KCl mixed solution in **Fig. S1**. We can see from **Fig. S1A**, the redox peaks of the GCE were weakest. While at the CDs/r-GO/GCE, the current of both anodic and cathodic peak were greatly increases, which were due to the modification of CDs/r-GO on GCE may greatly accelerate the electron transfer rate.[40] **Fig. S1B** shows the EIS of different electrodes. On the bare GCE the R_{et} value was 400 Ω. When r-GO was modified onto GCE surface, the R_{et} value dramatically increased to about 1560 Ω, suggesting that r-GO acted as an insulating layer which caused difficult at the interfacial electron transfer due to their disrupted sp^2 bonding networks.[41] While on the CDs/GCE the R_{et} value was decreased than bare electrode, indicated that the CDs on could accelerate the electron transfer rate. However, the R_{et} value increased to 1390 Ω on the CDs/r-GO modified GCE. The R_{et} value increased obviously illustrating the CDs was successful functionalization of r-GO and the CDs/r-GO modified GCE was obtained.

The electrochemical properties for different electrodes of GCE, r-GO/GCE and CDs/r-GO/GCE were studied in 0.1 M phosphate solutions. As illustrated in **Fig. 4,** the oxidation peak current of dihydroxybenzenes isomers increased significantly on CDs/r-GO/GCE. A possible reaction mechanism was discussed. As the electron collectors and transporters, some unoxidized aromatic rings of r-GO would provide a selective interface by hydrogen bonds and rich delocalized π electrons. After chemical reduced CDs and graphene oxide, the strong π-π stacking force, hydrogen bonding force and sp^2 and sp^3 hybrid structure could accumulate CDs around of the r-GO layers. At CDs/r-GO/GCE, the proton-donating groups of HQ, CC and RC molecule facilitated the charge transport rate, which significantly enhanced the corresponding peak current and exhibited improved catalytic separation performance of the coexisting HQ, CC and RC.

Fig. 4

3.3. Effects of scan rate and pH

In the following experiment, the electrochemical behaviors of hydroquinone, catechol and resorcinol (CV of 0.2 mM dihydroxybenzene isomers on the CDs/r-GO/GCE) were studied at various scan rates. As the scan rate increases, the oxidation peak current increased linearly well. The redox peak current was proportional to the scan rate in the range of 0.01-0.4 V s^{-1} was shown in **Fig. 5**. Moreover, with the increase of scan rate, the redox potential of HQ, CC and RC shifted positively. The oxidation peak currents (I_{pa}) shows a linear relationship with the scan rate (υ) whose equation is HQ I_{pa} (μA) = -131.62 υ (V s^{-1}) - 4.97 (R = 0.9969) and I_{pc} (μA) = 67.47 υ (V s^{-1}) + 1.04 (R = 0.9974). For CC, the I_{pa} (μA) = -147.18 υ (V s^{-1}) - 6.28 (R = 0.9967) and I_{pc} (μA) = 116.27 υ (V s^{-1}) + 3.71 (R = 0.9961). For RC, only an oxidation peak was observed, which proves once again that the oxidation process is a totally irreversible electrode process, the linear regression equations of RC can be expressed as I_{pa} (μA) = -136.33 υ (V s^{-1}) - 6.42 (R = 0.9963), which indicated that the redox of HQ, CC and RC on CDs/r-GO/GCE were typical adsorption-controlled processes.[42]

The effect of the pH value on the CV response of 0.2 mM dihydroxybenzene isomers on the CDs/r-GO/GCE was investigated and shown in **Fig. S2**. The reduction potential shifted negatively and the peak current keep basic consistent as the pH value increased until it reaches 7.0. However, upon further increase of the pH value, the reduction peak current decreased. In order to reduce the over-potential and enhance the electron transfer rate, pH 7.0 of PBS solutions was chose as the optimal value in this experiment.

Fig. 5

3.4. Differential pulse voltammetry simultaneous determination of HQ, CC and RC

Simultaneous detection of HQ, CC and RC were performed on the CDs/r-GO/GCE in 0.1 M phosphate solutions. As illustrated in **Fig. 6A**, with the increase of the HQ concentrations in the presence of 0.2 mM CC and 0.2 mM RC, the anodic peak currents of HQ were linearly increased ranging from 0.5 to 1000.0 μM, the equation was: I_{pa} (μA) = -0.045 C (μM) - 40.01 (R = 0.9964). Similarly, as shown in **Fig. 6B**, keeping the concentration of HQ and RC constant (0.2 mM), the oxidation peak current increased linearly with increasing the concentration of CC in the range of 1.0 to 950.0 μM, the equation: I_{pa} (μA) = -0.058 C (μM) - 23.90 (R = 0.9951). The DPVs of RC with different concentrations in the presence of 0.2 mM HQ and CC (**Fig. 6C**), the linear egression equation is calibrated as I_{pa} (μA) = -0.031 C (μM) - 17.78 (5.0 to 600.0 μM, R = 0.9973). The detection limits (S/N=3) for the detection of HQ, CC and RC were evaluated as 0.17 μM, 0.28 μM and 1.0 μM. Thus, the selective and sensitive determination of HQ, CC and RC were achieved simultaneously at CDs/r-GO/GCE. In addition, the peaks near -0.2 V have been shown in Fig. 6. The possible reason of the peaks near -0.2 V may be ascribed that characteristic peak of the incomplete reduction of the graphene oxide, the two close hydroxyl on the carbon dehydration to formed a cycle and then restored between the oxidation and reduction.

Fig. 6

3.5. Reproducibility and stability studies

The reproducibility and stability of the modified electrode were evaluated in these sensing studies. The relative standard deviation (RSD) for five measurements was 2.3%, suggesting the acceptable repeatability and precision. Moreover, the stability of the CDs/r-GO/GCE was checked in **Fig. S3**. The response of the modified electrode to 0.2 mM dihydroxybenzene isomers solution only decreased 2.63% of its initial response signal after being stored for 2 weeks, indicating good stability of the sensor. Moreover, Some common interference for the simultaneous determination of HQ, CC and RC were also investigated, such as $MgCl_2$, NaCl, K_2SO_4 solutions (100 fold), phenol, nitrophenol and glucose solutions (50 fold). The oxidation peak potential and current of HQ, CC and RC were observed almost constantly in the presence of all interferes. Thus, the results indicated the CDs/r-GO/GCE exhibited good selectivity for detection of dihydroxybenzene isomers.

3.6. Application of the method into the analysis of samples

The comparison of the proposed method with other electrochemical methods reported for the determination was shown in **Table 1**.[43] Wider linear range and lower detection limit of CDs/r-GO/GCE sensor for the simultaneous detection of HQ, CC and RC. For the further evaluation of the applicability of the method tap waters, local river water and industrial sewage samples were used for quantitative analysis after filtering with a cellulose membrane filter (pore size 0.25 μm) for several times. Then 5 mL of the real samples were diluted to 10 mL with 0.1 mM PBS solutions. The results were shown in **Table 2.** The recovery of the real samples ranged between 98.7% and 101.7% (n=6). The results indicated practical applicability of CDs/r-GO/GCE for simultaneous determination of HQ, CC and RC in real water samples.

Table 1

Table 2

4. Conclusions

In summary, the CDs/r-GO composite was designed and constructed as electrode materials. The support matrix r-GO straightforwardly combined with CDs and firstly was used as electrochemical sensor for simultaneous determination of HQ, CC and RC. The performance of the electrode was improved greatly compared with that of electrode modified by r-GO or CDs alone because of their unique chemical and electrochemical properties and their synergy effect. Detection limits for HQ, CC and RC were 0.17 μM, 0.28 μM and 1.0 μM (S/N=3), respectively. Excellent reproducibility and stability in practical water samples show that this novel composite can provide a promising platform for the quantitative detection of HQ, CC and RC in micromole level for real samples.

Acknowledgments

This project was supported by Fujian Province Natural Science Foundation (2012D136), the Science and Technology Foundation of Fujian Provincial Bureau Quality and Technical Supervision (NO.FJQI 2013108), National Undergraduate Innovative Training Program (201410402002).

References

1 M. Narmadha, M. Noel, V. Suryanarayanan, J. Electroanal. Chem., 2011, **655**, 103.

2 S. Palanisamy, C. Karuppiah, S. M. Chen, K. Muthupandi, R. Emmanuel, P. Prakash, M. S. Elshikh, M.A. Ali, F.M.A. Al-Hemaid, Electroanalysis, 2015, **27**, 1.

3 J. Qu, Y. Wang, Y. Dong, Z. Zhu and H. Xing, Anal. Methods, 2015, **7**, 260.

4 H. Yin, Q. Zhang, Y. Zhou, Q. Ma, T. liu, L. Zhu, S. Ai, Electrochim. Acta, 2011, **56**, 2748.

5 C. Zhang, L. Zeng, X. Zhu, C. Yu, X. Zuo, X. Xiao, J. Nan, Anal. Methods, 2013, **357**, 2203.

6 G. Marrubini, E. Calleri, T. Coccini, A.F. Castoldi, L. Manzo, Chromatographia, 2005, **62**, 25.

7 P. S. Selvan, R. Gopinath, V. S. Saravanan, N. Gopal, S. A. Kumar, K. Periyasamy, Asian J. Chem., 2007, **19**, 1004.

8 P. Nagaraja, R. A. Vasantha, K. R. Sunitha, Talanta, 2001, **55**, 1039.

9 P. R. Dalmasso, M. L. Pedano, G. A. Rivas, Sens. Actuators B: Chem., 2012, **173**, 732.

10 A. Navaee, A. Salimi, H. Teymourian, Biosens. Bioelectron., 2012, **31**, 205.

11 A. T. E. Vilian, S. M. Chen, L.H. Huang, M. A. Ali, F. AlHemaid, Electrochim. Acta, 2014, **125**, 503.

12 S. Wu, Q. He, C. Tan, Y. Wang, H. Zhang, Small, 2013, **9**, 1160.

13 R. K. Joshi, P. Carbone, F. C. Wang, V. G. Kravets, Y. Su, I. V. Grigorieva, H. A. Wu, A. K. Geim, R. R. Nair, Science, 2014, **343**, 752.

14 K. P. Loh, Q. Bao, P. K. Ang, J. Yang, J. Mater. Chem., 2010, **20**, 2277.

15 R. Song, W. Feng, C. A . Jimenez-Cruz, B. Wang, W. Jiang, RSC Adv., 2015, **5**, 274.

16 S. Bai, J. Ge, L. Wang, M. Gong, M. Deng, Q. Kong, L. Song, J. Jiang, Q. Zhang, Y. Luo, Y. Xie, Y. Xiong, Adv. Mater., 2014, **32**, 5689.

17 F. H. L. Koppens, T. Mueller, P. Avouris, A. C. Ferrari, M. S. Vitiello, M. Polini, Nat. Nanotechnol., 2014, **9**, 780.

18 F. Meng, X. Zhang, B. Xu, S. Yue, H. Guo, Y. Luo, J. Mater. Chem., 2011, **21**, 18537.

19 A. N. Aleshin, I. P. Shcherbakov, A. S. Komolov, V. N. Petrov, I. N. Trapeznikova, Organic Electronics, 2015, **16**, 186.

20 S. Hu, W. Zhang, J. Zheng, J. Shi, Z. Lin, L. Zhong, G. Cai, C. Wei, H. Zhang and A. Hao, RSC Adv., 2015, **5**, 18615.

21 X. Ma, Z. Liu, C. Qiu, T. Chen, H. Ma, Microchim. Acta, 2013, **180**, 461.

22 F. Hu, S. Chen, C. Wang, R. Yuan, D. Yuan, C. Wang, Anal. Chim. Acta, 2012, **724**, 40.

23 K. J. Huang, L. Wang, Y. J. Liu, T. Gan, Y. M. Liu, L. L. Wang, Y. Fan, Electrochim. Acta, 2013, **107**, 379.

24 Q. Liu, B. Guo, Z. Rao, B. Zhang, J.R. Gong, Nano Lett., 2013,**13**, 2436.

25 H. Li, X. He, Y. Liu, H. Huang, S. Lian, S. T. Lee, Z. Kang, Carbon, 2011, **49**, 605.

26 H. Li, Z. Kang, Y. Liu, S. T. Lee, J. Mater. Chem., 2012, **22**, 24230.

27 C.G. Joaquim, D.S. Esteves, M.R.G. Helena, Trends in Analytical Chemistry, 2011, **30**, 1327.

28 S. Qu, X. Wang, Q. Lu, X. Liu, L. Wang, Angew. Chem. Int. Ed., 2012, **51**, 12215.

29 J. C. G. Esteves da Silva, H. M. R. Goncalves, TrAC Trends Anal. Chem., 2011, **30**, 1327.

30 W. Kwon, S. W. Rhee, Chem. Commun., 2012, **48**, 5256.

31 Y. Li, Y. Zhong, Y. Zhang, W. Weng, S. Li, Sens. Actuators B: Chem., 2015, **206**, 735.

32 W. S. Hummers, R. E. Offeman, Journal of the American Chem. Soc., 1958, **80**, 1339.

33 X. Kang, J. Wang, H. Wu, I. A. Aksay, J. Liu, Y. Lin, Biosens. Bioelectron., 2009, **25**, 901.

34 G. Wang, ,B. Wang, J. Park, J. Yang, X. Shen, J. Yao, carbon, 2009, **47**, 68.

35 Q. Liang, W. Ma, Y. Shi, Z. Li, X. Yang, Carbon, 2013, **60**, 421.

36 C. Zhu, J. Zhai, S. Dong, Chem. Commun., 2012, **48**, 9367.

37 P. V. Kumar, N. M. Bardhan, S. Tongay, J. Wu, A. M. Belcher, J. C. Grossman, Nature Chemistry, 2014, **6**, 151.

38 S. N. Baker, G. A. Baker, Luminescent Carbon Nanodots: Emergent Nanolights, Angew. Chem. Int. Ed., 2010, **49**, 6726.

39 Q. Li, B. Guo, J. Yu, J. Ran, B. Zhang, H. Yan, J. R. Gong, J. Am. Chem. Soc., 2011, **133**, 10878.

40 H. Du, J. Ye, J. Zhang, X. Huang, C. Yu, Journal of Electroanalytical Chemistry 2011, **650**, 209.

41 Y. Hu, F. Li, X. Bai, D. Li, S. Hua, K. Wang, L. Niu, Chem. Commun., 2011, **47**, 1743.

42 X. Feng, W. Gao, S. Zhou, H. Shi, H. Huang, W. Song, Anal. Chim. Acta, 2013, **805**, 36.

43 L. Chen, Y. Tang, K. Wang, C. Liu, S. Luo, Electrochemistry Communications 2011, **13**, 133.

Figure and table captions

Fig. 1 SEM images of GO (A), TEM images of CDs. Inset: size distribution of CDs (B) and SEM images of CDs/r-GO (C).

Fig. 2 AFM images of GO/GCE (A), CDs/GCE (B) and CDs/r-GO/GCE (C).

Fig. 3 (A) UV-vis absorption spectra (Abs) and fluorescence spectra (Ex, Em) of the CDs intensity and (B) FT-IR spectra of CDs, GO, r-GO and CDs/r-GO.

Fig. 4 Cyclic voltammograms of 0.2 mM HQ, CC and RC at GCE, r-GO/GCE, CDs/GCE and CDs/r-GO/GCE.

Fig. 5 CV of 0.2 mM HQ, CC and RC on the CDs/r-GO/GCE at different scan rate (0.01, 0.03, 0.05, 0.075, 0.10, 0.15, 0.20, 0.25, 0.30, 0.35, 0.40 V s^{-1}). Inset: the redox peak current relation with the scan rate.

Fig. 6 DPVs of HQ concentrations: 0, 0.2 μM, 1.0 μM, 10 μM, 20 μM, 40 μM, 70 μM, 130 μM, 190 μM, 250 μM, 340 μM, 450 μM, 580 μM, 700 μM, 850 μM and 1000 μM. (B) DPVs of CC concentrations: 0, 1.0 μM, 5.0 μM, 10.0 μM, 40 μM, 70 μM, 100 μM, 150 μM, 200 μM, 260 μM, 350 μM, 450 μM, 600 μM, 750 μM and 900 μM. (C) DPVs of RC concentrations: 0, 5.0 μM, 20μM,50 μM, 70 μM, 100 μM, 160 μM, 250 μM, 340 μM, 460μM and 600 μM at CDs/r-GO/GCE in the presence of other two interfering substance (concentration 0.2 μM).

Table 1 Comparison of different electrochemical sensors for the determination of dihydroxybenzene isomers.

Table 2 Results of determination of dihydroxybenzene isomers in real samples.

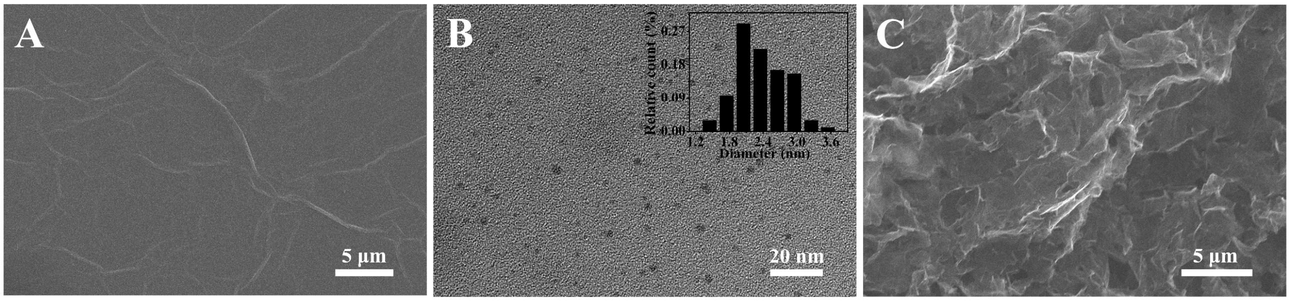
A
5 µm
B
Relative count (%)
0.27
0.18
0.09
0.00
1.2
1.8
2.4
3.0
3.6
Diameter (nm)
20 nm
C
5 µm

Fig. 1

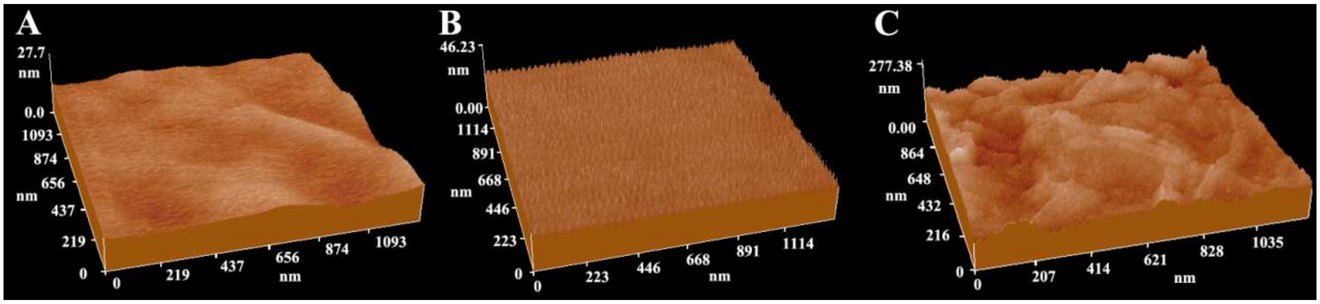
A
27.7 nm
0.0
1093
874
656
nm
437
219
0
0
219
437
656
874
1093
nm
B
46.23 nm
0.00
1114
891
668
nm
446
223
0
0
223
446
668
891
1114
nm
C
277.38 nm
0.00
864
648
nm
432
216
0
0
207
414
621
828
1035
nm

Fig. 2

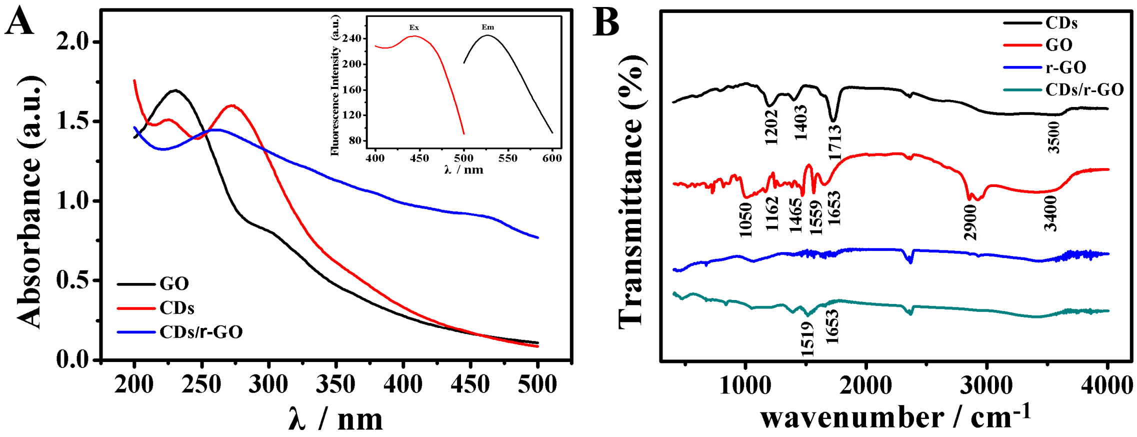
A
Absorbance (a.u.)
0.0
0.5
1.0
1.5
2.0
200
250
300
350
400
450
500
λ / nm
GO
CDs
CDs/r-GO
Fluorescence Intensity (a.u.)
80
120
160
200
240
Ex
Em
400
450
500
550
600
λ / nm
B
Transmittance (%)
CDs
GO
r-GO
CDs/r-GO
1202
1403
1713
3500
1050
1162
1465
1559
1653
2900
3400
1519
1653
1000
2000
3000
4000
wavenumber / cm-1

Fig. 3

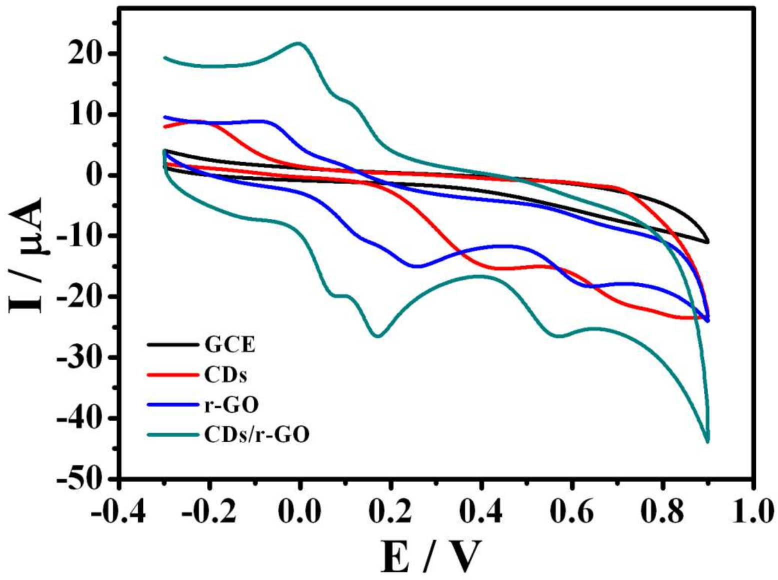
I / μA
20
10
0
-10
-20
-30
-40
-50
-0.4
-0.2
0.0
0.2
0.4
0.6
0.8
1.0
E / V
GCE
CDs
r-GO
CDs/r-GO

Fig. 4

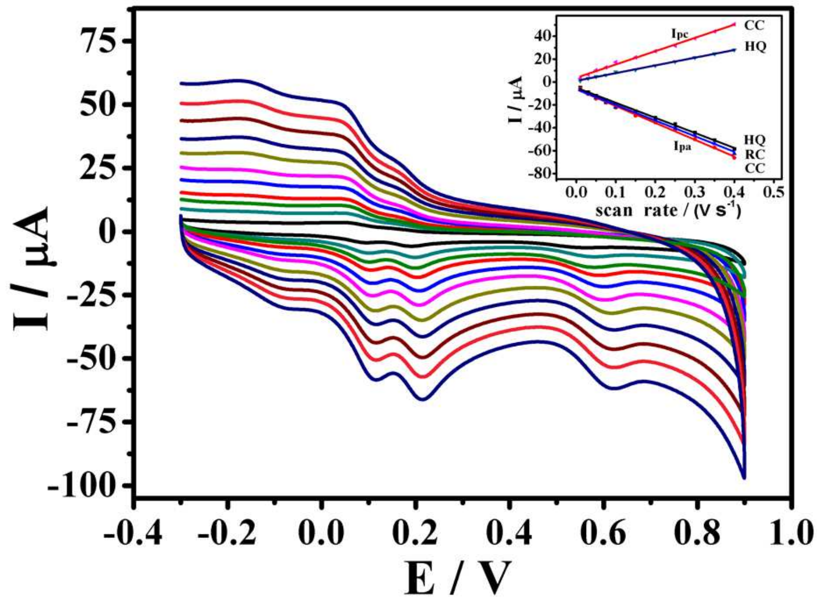
I / µA
E / V
75
50
25
0
-25
-50
-75
-100
-0.4
-0.2
0.0
0.2
0.4
0.6
0.8
1.0
I / µA
scan rate / (V s^{-1})
Ipc
Ipa
CC
HQ
HQ
RC
CC
40
20
0
-20
-40
-60
-80
0.0
0.1
0.2
0.3
0.4
0.5

Fig. 5

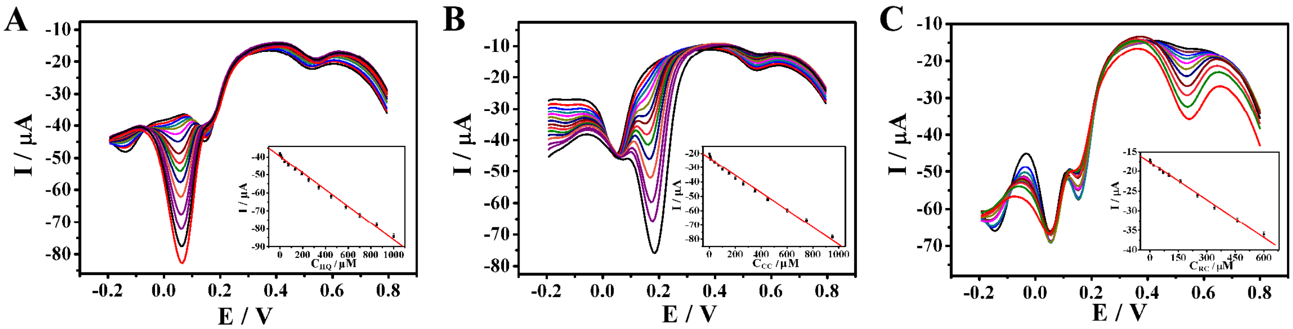
A
B
C
I / μA
E / V
-10
-20
-30
-40
-50
-60
-70
-80
-0.2
0.0
0.2
0.4
0.6
0.8
C_{HQ} / μM
C_{CC} / μM
C_{RC} / μM
0
200
400
600
800
1000
150
300
450
-15
-25
-35
-90

Fig. 6

Electrode	Linear (μM)			Detection limit (μM)			Ref.
	HQ	CC	RC	HQ	CC	RC	
Graphene-chitosan/GCE	1.0-400	1.0-550	1.0-300	0.75	0.75	0.75	4
CNF/GCE	6.0-200	2.0-200	-	0.25	0.1	-	5
Pt/ZrO_2-rGO/GCE	1.0-1000	1.0-400	-	0.4	0.4	-	11
r-GO-MWNTs/GCE	8.0-391	5.5-540	-	2.6	1.8	-	22
WS_2-graphene/GCE	1.0-100	1.0-100	1.0-100	0.1	0.2	0.1	23
EG/GCE	6-200	1-200	-	0.2	0.1	-	40
Graphene/GCE	1-500	1-500	-	0.015	0.01	-	43
CDs/r-GO/GCE	0.5-1000	1.0-950	5.0-600	0.17	0.28	1	This work

Table 1

samples	original(μM)			Added (μM)			Found (μM)			Recovery(%)		
	HQ	CC	RC	HQ	CC	RC	HQ	CC	RC	HQ	CC	RC
Tap water	0	0	0	100	100	100	100.6±0.5	101.3±0.4	99.2±0.9	100.9	101.5	98.7
River water	0	0	0	200	200	200	199.6±0.5	201.3±0.4	198.8±0.9	99.7	100.8	99.2
industrial sewage	230±1.9	85±1.3	15±1.1	100	100	100	328.2±2.6	185.9±2.4	115.8±2.1	99.1	101.2	101.7
				200	200	200	427.8±2.6	286.3±2.7	216.4±3.9	99.2	100.8	101.6

Table 2